

Effects of Intravenously Administered Recombinant Vesicular Stomatitis Virus (VSV Δ M51) on Multifocal and Invasive Gliomas

XueQing Lun, Donna L. Senger, Tommy Alain, Andra Oprea, Kelley Parato, Dave Stojdl, Brian Lichty, Anthony Power, Randal N. Johnston, Mark Hamilton, Ian Parney, John C. Bell, Peter A. Forsyth

Background: An ideal virus for the treatment of cancer should have effective delivery into multiple sites within the tumor, evade immune responses, produce rapid viral replication, spread within the tumor, and infect multiple tumors. Vesicular stomatitis virus (VSV) has been shown to be an effective oncolytic virus in a variety of tumor models, and mutations in the matrix (M) protein enhance VSV's effectiveness in animal models. **Methods:** We evaluated the susceptibility of 14 glioma cell lines to infection and killing by mutant strain VSV Δ M51, which contains a single-amino acid deletion in the M protein. We also examined the activity and safety of this strain against the U87 and U118 experimental models of human malignant glioma in nude mice and analyzed the distribution of the virus in the brains of U87 tumor-bearing mice using fluorescence labeling. Finally, we examined the effect of VSV Δ M51 on 15 primary human gliomas cultured from surgical specimens. All statistical tests were two-sided. **Results:** All 14 glioma cell lines were susceptible to VSV Δ M51 infection and killing. Intratumoral administration of VSV Δ M51 produced marked regression of malignant gliomas in nude mice. When administered systemically, live VSV Δ M51 virus, as compared with dead virus, statistically significantly prolonged survival of mice with unilateral U87 tumors (median survival: 113 versus 46 days, $P = .0001$) and bilateral U87 tumors (median survival: 73 versus 46 days, $P = .0025$). VSV Δ M51 infected multifocal gliomas, invasive glioma cells that migrated beyond the main glioma, and all 15 primary human gliomas. There was no evidence of toxicity. **Conclusions:** Systemically delivered VSV Δ M51 was an effective and safe oncolytic agent against laboratory models of multifocal and invasive malignant gliomas, the most challenging clinical manifestations of this disease. [J Natl Cancer Inst 2006;98:1546–57]

Human malignant glioma is one of the most common primary central nervous system tumors in adults. The ability to treat

patients with malignant gliomas remains poor. Despite dramatic improvements in neuroimaging and neurosurgical techniques, the prognosis of patients with malignant glioma has not improved substantially during the past 30 years (1). The most aggressive treatment available for patients with malignant glioma is surgical resection followed first by conventional radiotherapy administered with concomitant chemotherapy and then by adjuvant chemotherapy (2). Despite successful initial treatment of patients with malignant glioma, the median survival of patients with glioblastoma multiforme thus treated is just over 1 year (2), and virtually all patients die of recurrent disease (3–5).

Malignant gliomas are diffuse, highly invasive, and often multifocal. The core tumor is surrounded by a penumbra of invasive tumor cells that are detectable several centimeters away from the main tumor mass. These locally invasive glioma cells, which are often found at the margins of the tumor resection, are the most common site of malignant glioma recurrence. In addition, these invasive glioma cells activate several cellular signaling pathways that render them more

Affiliations of authors: Departments of Oncology, Clinical Neurosciences, and Biochemistry and Molecular Biology, Tom Baker Cancer Centre (XL, DLS, TA, AO, RNJ, IP, PAF), Clark H. Smith Integrative Brain Tumor Research Center (XL, DLS, TA, AO, MH, IP, PAF), Department of Neurosurgery (MH), University of Calgary, AB, Canada; Ottawa Regional Cancer Centre Research Laboratories, Ottawa, ON, Canada (KP, AP, JCB); Apoptosis Research Center, Children's Hospital of Eastern Ontario, Ottawa, ON, Canada (DS); Centre for Gene Therapeutics, Department of Pathology and Molecular Medicine, McMaster University, Hamilton, ON, Canada (BL).

Correspondence to: Peter A. Forsyth, MD, Clark H. Smith Integrative Brain Tumor Research Center, Rm. 372A, Heritage Medical Research Building, 3330 Hospital Dr. NW, Calgary, AB T2N 4N1, Canada (e-mail: pforseyth@ucalgary.ca). See "Notes" following "References."

DOI: 10.1093/jnci/djj413

© 2006 The Author(s).

This is an Open Access article distributed under the terms of the Creative Commons Attribution Non-Commercial License (<http://creativecommons.org/licenses/by-nc/2.0/uk/>), which permits unrestricted non-commercial use, distribution, and reproduction in any medium, provided the original work is properly cited.

resistant to conventional chemotherapies than their noninvasive counterparts (6). Therefore, malignant glioma must be considered as a cerebral disease that requires treatment not only of a single, main tumor mass but also of invasive cells and multiple tumor foci.

Recently, several oncolytic viruses have shown promising results in preclinical models of brain tumors. These viruses include reovirus (7–9), recombinant herpes simplex virus (10–14), Newcastle disease virus (15–17), recombinant poliovirus (18,19), myxoma virus (20), modified adenovirus (21–23), and wild-type vesicular stomatitis virus (VSV) (24–28). Despite impressive preclinical data, there are potential limitations to the use of these viruses in patients, such as inadequate distribution and/or delivery and insufficient levels of gene transfer or virus replication (29–32). Indeed, no dramatic results have been reported in the small number of early clinical trials in humans using oncolytic viruses against malignant glioma (15,16,33–36). Case reports of long-term survivors (35) and a patient with a complete response (17) have been described, and a clinical trial in patients with recurrent malignant gliomas treated with reovirus has been completed (37), but a final report has not been published.

Oncolytic viruses exploit a number of genetic defects in tumor cells (38–42). A common genetic defect occurring during tumor evolution is diminished responsiveness to interferon (43,44). This common defect reflects the important role of interferon-regulated pathways in the control of normal growth and apoptosis. Interferon is also a key mediator of the individual cell's innate antiviral response. When tumor cells acquire mutations that allow them to escape interferon-mediated growth control pathways (e.g., those controlling proliferation or apoptosis), the tumor cells simultaneously compromise their innate viral responses, permitting a lethal viral infection within the tumor cell. In addition, tumor cells may have defects in signaling pathways such as the Myc, Ras, or p53 pathways that render them susceptible to VSV replication (26,28,45). Thus, tumor cells undergo growth and proliferation at the expense of losing their resistance to viral infection, and a lethal oncolytic infection occurs.

We and others have found that wild-type VSV is a potent oncolytic virus in a number of tumor cell types, including gliomas (24,28,43–45) but is lethal to animals that have not been treated with interferon (43). Hence, we used a VSV mutant called VSV Δ M51. VSV Δ M51 has a single amino acid deletion of methionine-51 (M51) of the matrix (M) protein. One of the functions of the M protein is to block the nuclear to cytoplasmic transport of interferon-beta mRNA, thereby circumventing the cellular interferon response. The deletion of methionine-51 from the M protein of VSV Δ M51 abolishes this block and restores interferon-mediated responses in normal cells. This mutant theoretically has an improved therapeutic value (that is, safer but retaining the same efficacy) compared with wild-type VSV because it induces a marked interferon response in normal cells but retains its full oncolytic effect against tumor cells both *in vitro* and *in vivo* (43).

During the past several years of oncolytic virus development, it has become apparent that insufficient viral delivery can be a key limitation in the treatment of brain tumors (29,38,40,43). Direct inoculation of virus into a tumor may be advantageous in the treatment of localized tumor, but focal necrosis, tissue planes, and high intratumoral pressure will still limit viral distribution. Intravascular administration is an attractive alternative and may allow for multiple administrations over a long period of time. Although

an intact blood–brain barrier will affect delivery to the normal brain, the blood–tumor barrier is somewhat permeable and may provide a potential advantage over direct intratumoral inoculation in delivery to multifocal tumors and invasive tumor cells. In addition, intravascular injection is simpler, less expensive, and less invasive clinically than direct local delivery. A number of preclinical studies have shown that virus treatments can be delivered to brain tumors via intracarotid delivery (46–50), but only two studies have shown intravenous delivery of an oncolytic virus for the treatment of brain tumors (51,52). The systemic/vascular delivery of VSV mutants has previously been shown to be effective in animal models of cancer, including those that had already widely metastasized (43,53) or were multifocal (54).

In this study, we investigated the effects of intravenous delivery of VSV Δ M51 for the treatment of brain tumors. We carried out a detailed evaluation of the oncolytic properties of VSV Δ M51 *in vitro*, *in vivo*, and *ex vivo* in human malignant glioma surgical specimens. We also compared the effects of VSV Δ M51 to those of another oncolytic virus, reovirus. Reovirus has activity against experimental models of malignant glioma, but a small number of glioma cell lines are highly resistant to infection and killing by this virus (8,9).

MATERIALS AND METHODS

Cell Lines

Fourteen human glioma cell lines (U87, U118, U251, U343, U373, U563, SF126, SF188, SNB19, UC12, UC13, UC14, RG2, and 9L) and murine NIH3T3 and L929 fibroblast cells were purchased from the American Type Culture Collection (ATCC, Manassas, VA). HS68 human foreskin fibroblast cells were a gift from Karl Riabowol (University of Calgary, Canada). All cells were propagated in Dulbecco's modified Eagle medium/F12 (DMEM/F12, Hybri-care; ATCC, Manassas, VA) containing 10% fetal bovine serum (FBS) at 37 °C in a humidified, 5% CO₂ incubator. Each cell line was tested regularly for mycoplasma contamination.

Transfection of Glioma Cells With Red Fluorescent Protein

FuGene transfection reagent (Roche Diagnostic Co, Indianapolis, IN) and an expression plasmid containing red fluorescent protein (RFP) (Clontech, Palo Alto, CA) were used for transfection of a glioma cell line (U87) with RFP, as previously described (7). Briefly, FuGene transfection reagent and RFP:DNA vector were incubated together for 30 minutes at room temperature in serum-free media. The DNA mixture was applied to U87 cells for 4 hours at 37 °C in serum-free media. FBS was then added to a final concentration of 10%. Cells were grown at 37 °C and 5% CO₂, and the culture medium was changed daily. After 4 days, transfected cells were selected for G418 antibiotic resistance (400 µg/mL) and identified by fluorescent microscopy. RFP expression was found in more than 95% of cells as determined by fluorescence-activated cell sorting; this method confirmed the purity of the U87-RFP-expressing cells.

Viruses and Cell Infection

VSV Δ M51 is derived from the Indiana serotype of VSV and is propagated in Vero cells (African green monkey kidney cells).

VSV Δ M51 has a single amino acid deletion of methionine-51 of the M protein and contains an extra cistron that encodes green fluorescent protein (GFP) inserted between the G and L sequences. This recombinant genome was used to generate a replication-competent, GFP-expressing VSV clone (43). Dead virus was prepared by exposing live virus to ultraviolet (UV) irradiation for 1 hour. Reovirus serotype 3 (strain Dearing or T3D) was grown in L929 mouse fibroblast cells and purified as previously described (55); it was similarly UV inactivated to generate dead virus. Tumor or normal cells grown to 50%–60% confluence in 96-well plates were infected in 50 μ L of serum-free medium and incubated for 1 hour at 4 °C for reovirus or 37 °C for VSV Δ M51. Medium (150 μ L) was then added to each well, and cells were returned to 37 °C at 5% CO₂ for use in subsequent experiments.

3-(4,5-Dimethylthiazol-2-yl)-2,5-Diphenyl-2H-Tetrazolium Bromide Assay

Viability of tumor or normal cells infected as above with different doses (multiplicity of infection [MOI] = 0, 1, and 10) of VSV Δ M51 or reovirus-T3D was measured 24 hours (VSV Δ M51) and 72 hours (reovirus) after infection by 3-(4,5-dimethylthiazol-2-yl)-2,5-diphenyl-2H-tetrazolium bromide (MTT) assay, as previously described (55). Briefly, cells were incubated with MTT (1 mg/mL) at 37 °C and 5% CO₂ for 1 hour and lysed with dimethyl sulfoxide, and the absorbance was read with an ultra microplate reader (Bio-Tek Instruments, Inc, Burlington, VT).

Assays to Measure Cytopathic Effect of VSV Δ M51 or Reovirus Infection

All glioma and normal cell lines were seeded at 5×10^4 cells per well in six-well plates and incubated at 37 °C in 5% CO₂ overnight. After infection with live or dead VSV Δ M51 at an MOI of 1.0 or 10 for 24–72 hours, the cells were examined using a Zeiss inverted microscope (Axiovert 200M) mounted with a Carl Zeiss camera (AxioCam MRc, Carl Zeiss Inc, Thornwood, NY) to obtain both phase contrast and fluorescent images (using a fluorescein isothiocyanate filter to visualize virus-encoded GFP).

Western Blot to Detect Viral Proteins

All cell lines were seeded at 5×10^4 cells per well in six-well plates and incubated at 37 °C in 5% CO₂ overnight. Cells were then treated with either dead or live VSV Δ M51 virus at an MOI of 1. Twenty-four hours after infection, the cells were collected by scraping and were lysed in 500 μ L of lysis buffer (20 mM Tris pH 8.0, 136 mM NaCl, 10% glycerol, 1% NP40, 0.02% leupeptin, 0.5% aprotinin, and 1.5% sodium orthovanadate) for 20 minutes. Cellular debris was removed by low-speed centrifugation (1000g for 10 minutes) at 4 °C. Protein concentration of cell lysates was determined using the BCA protein assay kit (BioLynx, Inc, Brockville, ON, Canada). Supernatants were frozen at –80 °C for long-term storage. For electrophoresis, equal amounts of protein were separated on 7.5% sodium dodecyl sulfate–polyacrylamide gels and transferred to nitrocellulose membranes. Membranes were incubated with polyclonal anti-VSV antibody (1:1000) overnight at 4 °C, washed three times with 1 \times Tris buffered saline, and incubated for 1 hour with horseradish peroxidase (HRP)–conjugated secondary antibody (1:3000 dilution,

Biosciences, Amersham, Piscataway, NJ) at room temperature (John C. Bell, unpublished). Antibody binding was detected using an enhanced chemiluminescence reagent (Biosciences, Amersham) according to the manufacturer's instructions.

Mice

CD-1 nude mice (female, 6–8 weeks old) were purchased from Charles River Canada, Constant, PQ, Canada. Three to four mice were caged together in each vivarium with a 12-hour light/dark schedule at 22 ± 1 °C and a relative humidity of $50 \pm 5\%$. Food and water were available ad libitum. In all experiments, mice were killed by cervical dislocation when they had difficulty ambulating, feeding, or grooming or had lost at least 20% of their body weight. All animal procedures were reviewed and approved by the University of Calgary Animal Care Committee.

In Vivo Oncolysis in Subcutaneous Tumor Model

Female CD-1 nude mice (n = 21) were each implanted with 1×10^6 U87 (n = 11) or U118 (n = 10) malignant glioma cells on the right flank to establish subcutaneous tumors. Tumor size (length \times width) was measured daily using calipers. When palpable tumors reached approximately 25 mm², mice were treated intratumorally with live or dead VSV Δ M51 virus (three injections of VSV Δ M51 1×10^7 plaque-forming units [PFU] at 2-day intervals) (8). Tumor size was then measured until sacrifice was indicated.

Determination of the Toxicity of the Intracerebral Administration of VSV Δ M51 in Nude Mice

Female CD-1 nude mice (n = 8) were injected intracerebrally with either dead or live VSV Δ M51 (5×10^2 , 1×10^3 , 1×10^4 PFU per mouse, two mice per dose) at a depth of 3 mm under guidance of a stereotactic frame (Kopf Instruments, Tujunga, CA), as described previously (7,20,56). Briefly, virus was injected intracerebrally into the right putamen. A 0.5-mm burr hole was made 1.5–2 mm right of the midline and 0.5–1 mm posterior to the coronal suture through a scalp incision. Stereotactic injection used a 5- μ L syringe (Hamilton Co, Reno, NV) with a 30-gauge needle, inserted through the burr hole to a depth of 3 mm, mounted on a Kopf stereotactic apparatus (Kopf Instruments). After 10 seconds, the needle was withdrawn and the incision was sutured. Mice were followed daily for toxic effects. After the mice were killed, their brains, lungs, kidneys, hearts, and livers were removed, fixed in 10% formalin, embedded in paraffin, and sectioned with a microtome. Sections were stained with hematoxylin and eosin for histologic analysis, analyzed for VSV antigens by immunohistochemistry, or analyzed for the presence of DNA fragments by terminal transferase deoxyuridine triphosphate nick-end labeling (TUNEL) assay.

Immunohistochemistry to Detect VSV Antigens

Frozen sections of mouse brain and major organs (heart, liver, lung, and kidney) were fixed in 4% paraformaldehyde for 20 minutes and washed three times in phosphate-buffered saline (PBS). Sections were then exposed to primary polyclonal rabbit anti-VSV antibody at a 1:3000 dilution in PBS containing 2%

bovine serum albumin, for 24 hours at 4 °C. Biotinylated anti-rabbit IgG (Vector Laboratories, Burlingame, CA) was used as the secondary antibody. Sections were then incubated with avidin conjugated to HRP (Vectastain ABC immunohistochemistry kit, Vector Laboratories), and staining was visualized by addition of the DAB (3,3'-diaminobenzidine) substrate. To visualize VSV antigens, sections were mounted and viewed with a Zeiss inverted microscope (Axiovert 200M) and a Carl Zeiss camera (AxioCam MRc) to obtain both phase contrast and fluorescent images.

TUNEL Assay

The presence of fragmented DNA was analyzed with the TUNEL technique using the ApopTag plus fluorescein in situ apoptosis detection kit (Chemicon, Inc, Temecula, CA) according to the manufacturer's instructions. Briefly, paraffin-embedded brain sections were dewaxed in xylene, rehydrated in an ethanol gradient, and treated with proteinase K (Invitrogen, Carlsbad, CA; 20 µg/mL in PBS) for 20 minutes at room temperature. Sections were washed in PBS, incubated with reaction mixture including terminal deoxynucleotidyl transferase and fluorescein-dUTP for 1 hour at 37 °C, washed in PBS, incubated with the antidigoxigenin conjugate for 30 minutes at 37 °C, and then counterstained with 4'-6-diamidino-2-phenylindole.

Sequencing of M Protein in VSV^{ΔM51}

At 48 hours after intracerebral injections of 1×10^4 PFU of VSV^{ΔM51}, mice were killed by cervical dislocation and their brains were homogenized in PBS (pH 7.2). Virus was amplified by a single passage of brain homogenate on Vero cells for 24 hours. Virions were purified from the Vero cell supernatant by passage through a 0.2-µm filter followed by centrifugation at 30 000g for 90 minutes. The virus pellet was resuspended in PBS, and genomic RNA was extracted by sequential addition of Trizol (Invitrogen) and chloroform (57), except that rather than lysing and extracting RNA from the cells, we extracted it from purified VSV particles. Samples were then centrifuged at 10 000g for 10 minutes, and the aqueous phase was removed and washed on an RNEasy spin column (Qiagen, Mississauga, Ontario, Canada) per the manufacturer's instructions. The RNA product was used as a template in a random hexamer-primed reaction using Superscript II reverse transcriptase to generate single-stranded viral cDNA. From this cDNA template, specific primers (sense: ACGAATTCAAATTAGGGATCGCACCACC, antisense: ACGGATCCCGTGATACTCGGGTTGACCT) were used in the polymerase chain reaction to amplify a 377-bp fragment spanning bases 61–438 of the VSV M gene. This product was purified on an agarose gel and sequenced directly from the above sense primer using an Applied Biosystems 3730 DNA Analyzer (Ottawa Genomics Innovation Centre).

Determination of the Appropriate VSV^{ΔM51} Dose for Intravenous Administration in Nude Mice

Female CD-1 nude mice (n = 24) received intravenous injection of dead or live virus (at doses of 5×10^7 , 5×10^8 , 1×10^9 , or 5×10^9 PFU per mouse) via the tail vein. Mice were followed for up to 60 days, and their body weights were recorded every other day. After the mice were killed by cervical dislocation, their

brains and major organs (liver, lung, heart, and kidney) were saved either for virus recovery assays in liquid nitrogen or pathologic analysis in formalin as described above. For the in vivo therapeutic experiments, we selected a dose that was one dose level below the dose at which 50% of the mice died; we refer to this dose as the maximum tolerated.

Virus Recovery Assays

Mice were killed by cervical dislocation, and saline was immediately infused into the left ventricle of the heart. Tissues were extracted and then homogenized in liquid nitrogen using a Pellet Pestles Kit (VWR International, Edmonton, Alberta, Canada) followed by repeated freeze–thawing to release virus from the cells. Supernatants were used for plaque titration on Vero cells as previously described (58). Briefly, Vero cells were plated in six-well plates and infected with serial dilutions of sample supernatant. Forty-eight hours after incubation at 37 °C in 5% CO₂, cells were overlaid with 2× MEM (Mediatech, Herndon, VA) and 2× Noble agar (Difco Laboratories, Detroit, MI) containing 0.2 mL neutral red (Sigma Chemical, Oakville, Ontario, Canada). Virus plaques were counted, and PFU were calculated by the number of plaques multiplied by the dilution factor.

Survival Studies in an Orthotopic Human Glioma Model of Nude Mice

To investigate the antitumor efficacy of VSV^{ΔM51} in mice, an orthotopic unilateral glioma animal model was established with the human glioma cell line U87. The stereotactic techniques used to implant glioma cells in the right putamen have been described previously (7,20). Briefly, female CD-1 nude mice (n = 13) were anesthetized, and U87 glioma cells (1×10^5 cells per mouse) were implanted under the guidance of a stereotactic frame, as described above. After 15 days, mice were injected intravenously via the tail vein with multiple doses of live (n = 8) or dead (n = 5) virus (5×10^8 PFU per mouse every 2 days, for a total of three injections). Mice were monitored every other day for survival. After the mice were killed, their brains and major organs were prepared as described above for histologic analysis, immunohistochemical analysis of VSV antigen, and TUNEL assay to assess apoptosis.

Survival was also assessed in mice with bilateral brain tumors. To prepare these mice, we implanted U87 cells (5×10^4 cells per mouse per side in both sides of the brain) in CD-1 nude mice (n = 11). After 11 days, mice were injected intravenously, via the tail vein, with live (n = 6) or dead (n = 5) virus (5×10^8 PFU per mouse) every other day for three injections and every 5 days for another three injections for a total of six injections. Survival was followed, and organs were analyzed as above.

VSV^{ΔM51} Viral Distribution Studies

To determine if VSV^{ΔM51} targets multifocal gliomas in the brain, we established a dual tumor model using U87 tumor cells. Cells were implanted by stereotactic techniques as described above in CD-1 nude mice (n = 18). After 15 days, each mouse was injected intravenously, via the tail vein, with a single dose of VSV^{ΔM51} (5×10^8 PFU per mouse). Mice were killed at the following time points after virus injection (three mice at each time

point): 0 hour, 10 hours, 24 hours, 72 hours, 7 days, and 15 days. After sacrifice by cervical dislocation, a whole brain picture was taken with a Leica MZ-FLIII fluorescence stereomicroscope using a standard GFP filter set (6,20). Photoshop 6.0 (Adobe) was used to process the images. After imaging, the brain and other major organs were removed and frozen in liquid nitrogen for virus recovery assays.

To determine the ability of VSV Δ M51 to target invasive cells, we implanted U87-RFP cells (3×10^5 per mouse) into the brains of mice ($n = 6$) to generate tumors. After 15 days, we injected VSV Δ M51 (5×10^8 PFU per mouse) intravenously, via the tail vein, into tumor-bearing mice. After 72 hours, mice were perfused with 5 mL of saline and killed by cervical dislocation. The brains were removed and embedded in OCT embedding medium. RFP-expressing tumors and GFP-labeled viruses were visualized in frozen brain sections by a Zeiss inverted microscope (Axiovert 200M) with a fluorescent GFP or rhodamine filter set (20). Immunohistochemical staining of VSV antigen was performed on tissue sections. A Carl Zeiss camera (AxioCam MRc) was used to obtain both phase contrast and fluorescent images of the tumor cell-expressed RFP and the virus-expressed GFP.

Primary Human Glioma Culture

Short-term cultures were established from patient samples of human gliomas ($n = 15$) obtained following brain tumor surgery at the Foothills Hospital (Calgary); this study was approved by the Conjoint Medical Ethics Committee. Briefly, each patient specimen was split in two pieces; one portion of the specimen was fixed in 10% formalin and the other portion of the specimen was used for short-term cultures. The tumor tissue that was used to establish short-term cultures was washed several times in sterile saline, transferred to a 35-mm tissue culture dish, cut into small pieces (approximately 0.5–1 mm in diameter), and dissociated with trypsin (0.25%) and 50 μ g/mL deoxyribonuclease (Roche Diagnostics, Laval, PQ, Canada) for 30 minutes at 37 °C. After filtering and washing with DMEM/F12 (containing 20% FBS), cells were resuspended in 20% FBS in DMEM/F12 and plated (at 10 000–100 000 cells per well) in 96-well plates. Cells were infected the following day with VSV Δ M51 virus, both live and UV inactivated, at MOIs of 0.1, 1, and 10. Cell viability was measured 72 hours later by MTT and cytopathic effect assays [as above and in (20)].

Primary Tumor Immunocytochemistry for Glial Fibrillary Acid Protein Expression

Primary tumor cells obtained from surgical specimens were grown in eight-well chamber slides (50 000–200 000 cells per well) and fixed for 15 minutes in 4% paraformaldehyde. Cells were then blocked with 10% goat serum and 0.1% Triton X-100 in PBS for 30 minutes. Primary antibody (glial fibrillary acidic protein [GFAP] monoclonal antibody 1:1000, Chemicon, Inc) was then added. After 24 hours at 4 °C, cells were washed with PBS and then incubated with anti-mouse IgG-Cy3 (Vector Laboratories) for 1 hour. Sections were mounted with Geltol mounting medium (Fisher scientific Co, Pittsburgh, PA) and viewed with a Zeiss microscope (Axiovert 200M), and pictures were taken with a Zeiss inverted microscope and a Carl Zeiss camera (AxioCam MRC).

Statistical Analyses

Statistical Analysis Software (SAS Institute, Inc, Cary, NC) and GraphPad Prism (version 4; GraphPad Software Inc, San Diego, CA) were used for statistical analyses. Survival curves were generated by the Kaplan–Meier method. The log-rank test and two-way analysis of variance (ANOVA) were used to compare the effect of different forms of treatment (live virus versus dead virus) and the time since administration on tumor size. All reported *P* values were two-sided and were considered to be statistically significant at *P* < .05.

RESULTS

Susceptibility of Human Malignant Glioma Cell Lines to Infection and Killing by VSV Δ M51

Fourteen malignant glioma cell lines were tested for susceptibility to infection and killing by VSV Δ M51 and reovirus T3D by cytopathic effect and MTT assays (representative examples in Fig. 1). All 14 cell lines were susceptible to infection and killing by VSV Δ M51, whereas only 12 (85%) of the lines were susceptible to infection and killing by reovirus (U118 and U343 were resistant). In contrast, neither of the normal cell lines tested (HS68 and NIH3T3) was killed by VSV Δ M51 or reovirus. Cells were infected with either 1 MOI of VSV Δ M51 or 10 MOI of reovirus; complete cell death was observed in all glioma cell lines 48 hours after infection with VSV Δ M51 (Fig. 1, A) but not until 144 hours after infection with reovirus (Fig. 1, B). Untreated cells and cells treated with UV-inactivated (dead) virus did not exhibit any cytopathic effect at any time point assessed.

The MTT viability assay confirmed the results from the cytopathic effect assays (Fig. 1, C). VSV Δ M51 produced more rapid glioma cell killing and at a lower (1 MOI, 24 hours) MOI than reovirus T3D (10 MOI, 72 hours) (Fig. 1, C). Extensive cell killing was found in all glioma cell lines in the presence of VSV Δ M51. The normal cell lines NIH3T3 and HS68 were not susceptible to either reovirus or VSV Δ M51 (Fig. 1, C). To ensure that cell killing following treatment with VSV Δ M51 was due to viral infection rather than a nonspecific effect, viral protein production was assessed by western blotting. All glioma lines exhibited viral protein production 24 hours after infection, in accordance with their susceptibility to killing by VSV (Fig. 1, D), whereas no viral protein production was seen in normal cell lines (Fig. 1, D).

Effects of Intratumoral Administration of VSV Δ M51 on a Glioma Cell Line Resistant to Infection by Reovirus

We next investigated if VSV Δ M51 would infect and kill a cell line resistant to reovirus in a subcutaneous tumor in CD-1 nude mice. We treated mice bearing subcutaneous human malignant glioma xenografts of U87 (susceptible to reovirus) and of U118 (resistant to reovirus). These cells were implanted in the hind flanks of mice, which were treated intratumorally with live or dead virus after palpable tumors had formed (1×10^7 PFU per mouse, every other day, for a period of 6 days). We observed statistically significant inhibition of tumor growth in the live virus-treated mice compared with the dead virus-treated control mice bearing either U87 (ANOVA, *P* < .0001) (Fig. 2, A) or U118 (two-way ANOVA, *P* < .0001) tumors (Fig. 2, B).

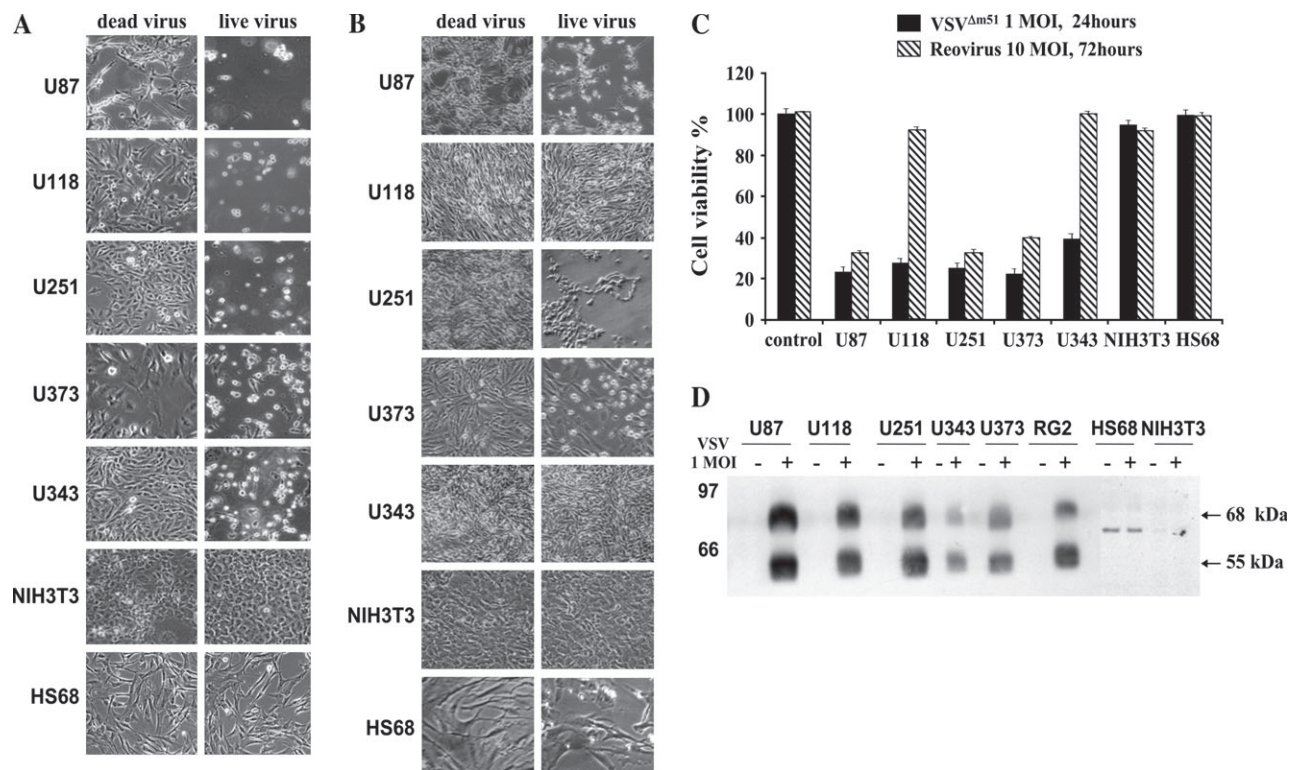


Fig. 1. Effects of vesicular stomatitis virus strain Δ M51 (VSV Δ M51) and reovirus T3D in vitro on established human malignant glioma cell lines. **A)** Cytopathic effects on glioma (U87, U118, U251, U373, U343) and normal (NIH3T3, HS68) cell lines of dead and live VSV Δ M51 at multiplicity of infection (MOI) = 1, 48 hours after infection (magnification: \times 100). **B)** Cytopathic effects on the same cell lines of dead and live reovirus at 10 MOI, 144 hours after infection, when the

full cytopathic effect of reovirus was produced (magnification: \times 100). **C)** 3-(4,5-Dimethylthiazol-2-yl)-2,5-diphenyl-2H-tetrazolium bromide assay comparing the effects of VSV Δ M51 or reovirus on the viability of glioma cell lines (U87, U118, U251, U373, U343) and normal cell lines (NIH3T3, HS68); ultraviolet-inactivated viruses were used as a negative control. **D)** Detection of VSV proteins by western blot after infection of glioma cell lines with VSV Δ M51.

Toxicity of Intracerebrally Administered VSV Δ M51 in CD-1 Nude Mice

We evaluated the toxicity of VSV Δ M51 in vivo when administered intracerebrally. A single intracerebral administration of VSV Δ M51 was lethal, even at a dose as low as 5×10^2 PFU per mouse (Fig. 3, A). This experiment was repeated three times with similar results (data not shown). Following intracerebral administration we found a diffuse meningoencephalitis, a marked tropism for neurons, and neuronal apoptosis. This was severe in the hippocampus (Fig. 3, B) and brain stem (data not shown), and the affected areas were positive for VSV antigen expression and TUNEL staining (Fig. 3, B).

We were surprised that the mutant VSV Δ M51, which was engineered to enhance the antiviral responses in normal cells, retained substantial neurotoxicity when administered intracerebrally. To exclude the possibility that the VSV Δ M51 had reverted to wild-type VSV (i.e., lost the mutation in the M protein), we sequenced the M protein of virus collected from mice after intracerebral administration. We confirmed that the virus cultured from the brains retained the mutation in the M protein and had not reverted to wild-type VSV.

Safety Evaluation of Intravenous Administration of VSV Δ M51 in Nude Mice

We next evaluated the toxicity and maximum tolerated dose of VSV Δ M51 administered intravenously. The mice tolerated

much higher doses of intravenously than intracerebrally administered VSV Δ M51. All mice ($n = 4$ per group) administered intravenously, via the tail vein, with doses of $\leq 1 \times 10^9$ PFU survived and appeared normal for up to 60 days (Fig. 4, A), when we terminated the experiment by killing all mice that were still alive. At a dose of 5×10^9 PFU (the highest dose we were technically capable of preparing), however, only 50% (two of four) of the mice survived for 60 days (Fig. 4, A). A transient and not statistically significant weight loss was observed 3–11 days after intravenous virus administration in surviving mice of both the 5×10^9 PFU and the 1×10^9 PFU groups (Fig. 4, B). Control mice treated with dead virus appeared normal. Hence, 1×10^9 PFU was the maximum tolerated dose when administered intravenously, and we used one dose level below this dose for all subsequent therapeutic experiments.

The histology of major organs (brain, liver, lung, kidney, and heart) of mice treated with a dose of 5×10^8 PFU was normal, and there was no histologic evidence of apoptosis by TUNEL assay (data not shown). In addition, we detected no viral antigen expression in liver, lung, kidney, or heart by immunohistochemistry, although in the brain there was minor VSV antigen staining within the meninges or ventricle at 24 and 72 hours after intravenous administration of virus (data not shown). Similar results were obtained by virus recovery assay. Virus was detected in the brain (but not in any other organs) only beginning 4 hours after intravenous administration, peaking at 24 hours, and declining thereafter (data not shown).

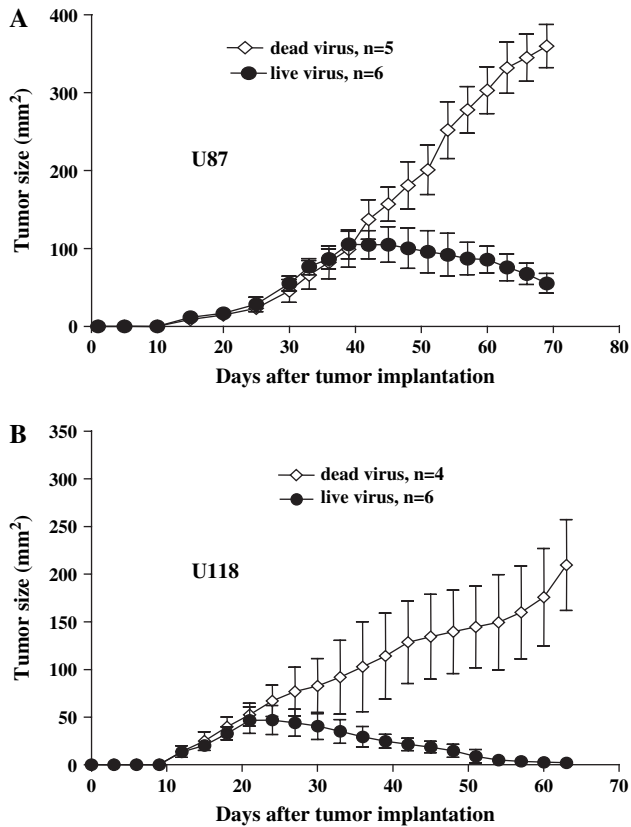


Fig. 2. Effects of vesicular stomatitis virus strain $\Delta M51$ ($VSV^{\Delta M51}$) on growth of reovirus-susceptible (U87) and reovirus-resistant (U118) glioma in a subcutaneous model of malignant gliomas in CD-1 nude mice. Mice bearing subcutaneous glioma implants were treated intratumorally with live or dead $VSV^{\Delta M51}$ virus when a palpable tumor reached approximately 25 mm²; tumor size (length \times width) was measured using a caliper. **A**) U87-derived gliomas, live virus (closed circles, n = 6) versus dead virus (open diamonds, n = 5). **B**) U118-derived gliomas, live virus (closed circles, n = 6) versus dead virus (open diamonds, n = 4). Results shown are the means and 95% confidence intervals of the tumor size.

Survival Following Systemic Intravenous Administration of $VSV^{\Delta M51}$ in CD-1 Nude U87 Tumor-Bearing Mice

We evaluated the effect of $VSV^{\Delta M51}$ delivered intravenously to mice with unilateral or bilateral brain tumors. Unilateral or bilateral U87 glioma orthotopic xenograft models were established by intracerebral inoculation of U87 cells into the brains of CD-1 nude mice. Mice were treated intravenously with multiple doses of $VSV^{\Delta M51}$ either 15 days (for unilateral tumors) or 11 days (for bilateral tumors) after tumor implantation. Mice with unilateral tumors treated with live virus survived statistically significantly longer (mean = 113 days, 95% CI = 96 to 130 days) than those treated with dead virus (mean = 46 days, 95% CI = 39 to 53 days, log-rank test, $P = .0001$) (Fig. 5, A). All mice eventually died from recurrent tumors between 35 and 140 days after tumor implantation. Similar, although less dramatic, results were found in mice harboring bilateral U87 human malignant gliomas. The median survival of dead versus live virus-treated mice was 46 versus 73 days, respectively (difference = 27 days, 95% CI = 38 to 54 days, and 95% CI = 62 to 84 days, respectively, log-rank test, $P = .0025$; Fig. 5, B). Similar results were obtained when these experiments were repeated (data not shown).

Histologic analysis showed that all live virus- and dead virus-treated mice died from a large tumor in the brain, with some live

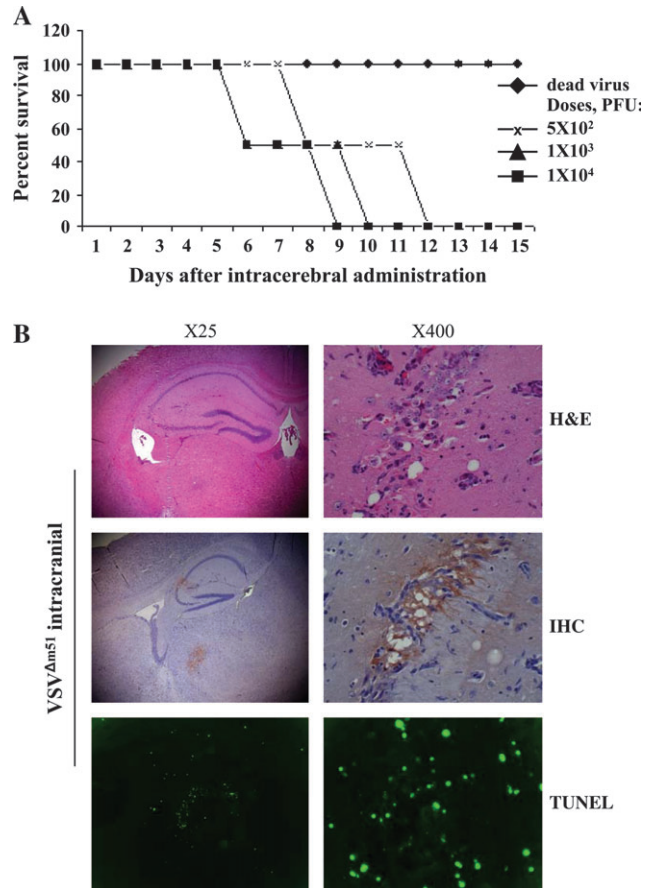


Fig. 3. Determination of the maximum tolerated intracerebral dose of vesicular stomatitis virus strain $\Delta M51$ ($VSV^{\Delta M51}$). **A**) Intracerebral administration: Normal CD-1 nude mice received a single administration of either ultraviolet-inactivated (dead virus) $VSV^{\Delta M51}$ or live $VSV^{\Delta M51}$ at doses of 5×10^2 , 1×10^3 , or 1×10^4 plaque-forming units (PFU) per mouse, two mice per dose. Mice were monitored for a period of 20 days. **B**) Neurotoxicity in mouse brain treated with $VSV^{\Delta M51}$ (1×10^4 PFU per mouse) administered intracerebrally (magnification: $\times 25$ and $\times 400$). Representative images show mouse brain stained for hematoxylin and eosin (H&E) (top row), by immunohistochemistry (IHC) for VSV antigen (middle row), and by terminal transferase deoxyuridine triphosphate nick-end labeling (TUNEL) assay (bottom row). Right column is a higher-magnification view of the hippocampus region of the brain.

virus-treated mice having slightly larger ventricles than dead virus-treated mice (data not shown). There was no histologically evident change in the hippocampus region of the brain, immunohistochemical staining evidence of viral infection of the hippocampus, or evidence of apoptosis by TUNEL staining of the hippocampus (Fig. 5, C).

Infection of Multifocal Gliomas and Invasive Tumor Cells With Intravenous $VSV^{\Delta M51}$

Having shown that intravenous $VSV^{\Delta M51}$ prolonged survival of mice bearing gliomas, we evaluated whether a productive infection occurred in the tumors and characterized the distribution of infection in the tumor margin and invasive glioma cells. Mice (n = 18) were implanted in both brain hemispheres with U87 cells and were administered a single intravenous dose of 5×10^8 PFU per mouse GFP-labeled $VSV^{\Delta M51}$ 15 days after tumor implantation. Mice were killed at multiple time points (three mice per time point), and their brains were examined in detail.

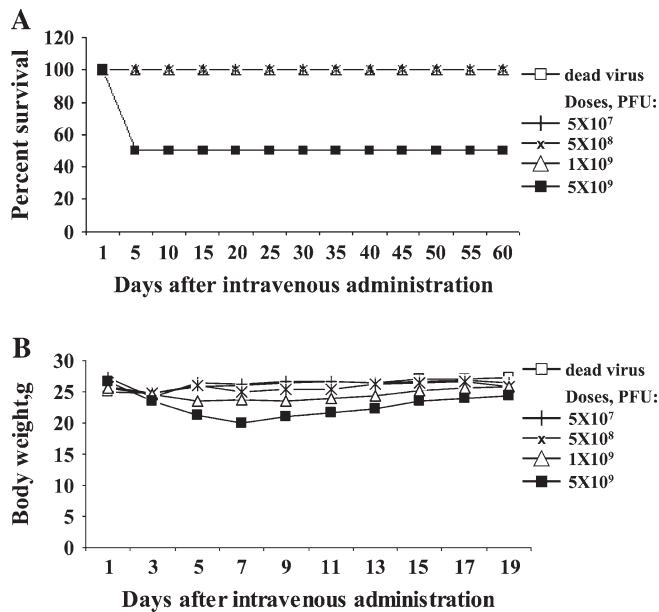


Fig. 4. Safety and toxicity evaluation of vesicular stomatitis virus strain $\Delta M51$ (VSV $\Delta M51$) when administered intravenously to nude mice. **A)** Intravenous administration of VSV $\Delta M51$ in CD-1 nude mice at doses of 5×10^7 , 5×10^8 , 1×10^9 , or 5×10^9 plaque-forming units (PFU) per mouse ($n = 4$ per group). Mice were given a single injection of dead or live VSV $\Delta M51$ intravenously, via the tail vein, and monitored for 60 days. **B)** Mean body weight over time of mice intravenously administered VSV $\Delta M51$.

GFP-expressing virus, as visualized by fluorescence microscopy, was confined to the tumor, with no expression elsewhere in the normal brain, lung, kidney, liver, or heart. Viral expression of GFP began 10 hours after infection, increased up to 72 hours, decreased slightly by day 7, and was undetectable by 15 days after viral administration (Fig. 6, A). The viral titers from the tumor tissues, as determined by virus recovery assays (Fig. 6, B), confirmed that a productive viral infection occurred in these tissues and that the infection had a similar temporal profile to the results based on fluorescence microscopy. No evidence of replicating virus was found in non-tumor-containing brain tissue (data not shown) or dead virus-treated brains (data not shown).

To determine whether VSV $\Delta M51$ infects invasive glioma cells that have migrated beyond the main glioma mass, we inoculated U87 cells that had been transfected with an expression plasmid containing RFP into the brains of six CD-1 nude mice. Fifteen days after implantation, a single intravenous dose of VSV $\Delta M51$ was administered, and (based on the in vivo viral distribution results above) the mice were killed 72 hours later. We then examined the sections of the brain using fluorescence microscopy and immunohistochemistry. We found that viral GFP colocalized with the tumoral RFP using fluorescence microscopy and colocalization of VSV proteins and tumor cells by immunohistochemistry (Fig. 6, C). In addition, viral GFP expression colocalized with isolated invasive tumor cells at the margins of the tumor (Fig. 6, C).

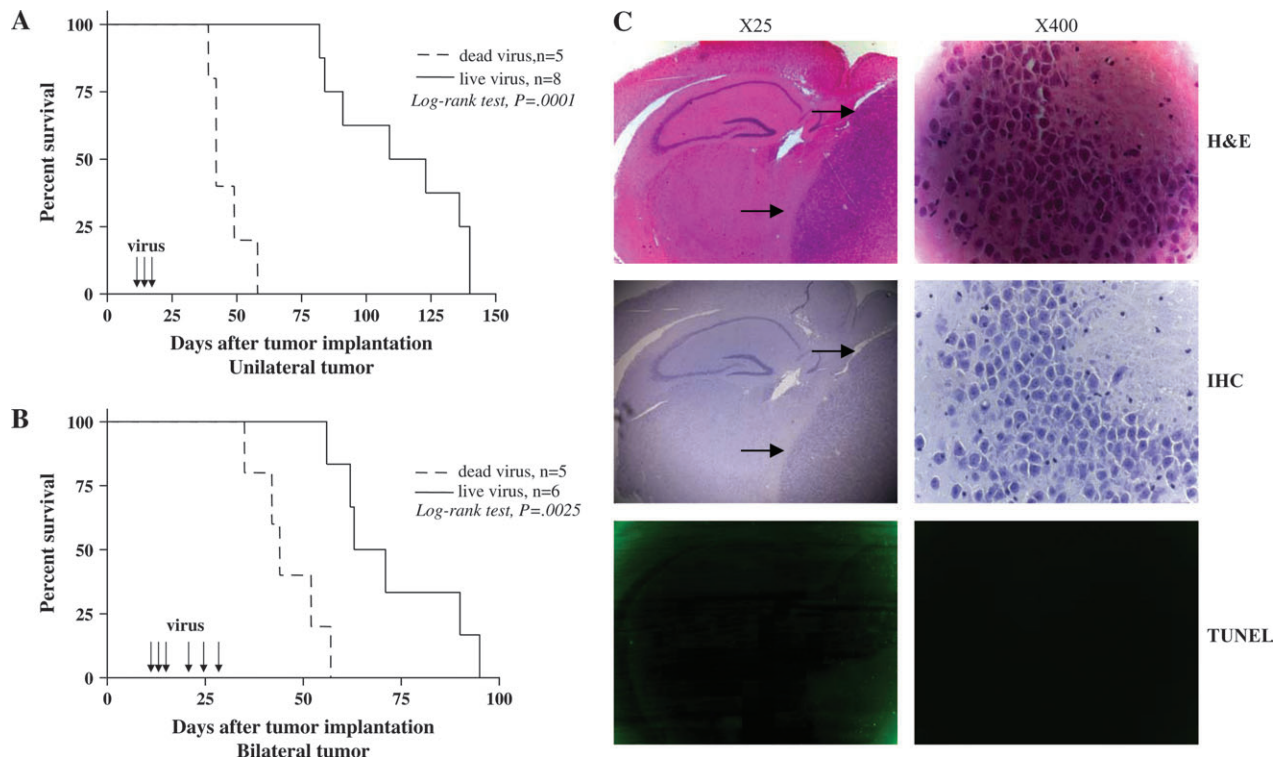


Fig. 5. Systemic administration of vesicular stomatitis virus strain $\Delta M51$ (VSV $\Delta M51$) and survival of nude mice with unilateral and bilateral U87 cell-derived brain tumors. **A)** Unilateral tumor model. Kaplan-Meier survival analysis of mice implanted with U87 cells (1×10^5 cells per mouse) and treated with either dead ($n = 5$) or live ($n = 8$) virus every 2 days for a total of three doses. One intravenous injection contained 5×10^8 plaque-forming units (PFU) per mouse. All P values are two-sided. **B)** Bilateral tumor model. Kaplan-Meier survival analysis of mice implanted with U87 cells (5×10^4 cells per mouse per side) and injected with either dead ($n = 5$) or live ($n = 6$) virus (5×10^8 PFU per

mouse three times every 2 days followed by three times every 5 days for a total of six injections. All P values are two-sided. **Arrows** in (A) and (B) indicate virus injections. **C)** Representative photomicrographs of a whole brain slice from a live virus-treated mouse (magnification: **left**, $\times 25$; **right**, $\times 400$). **Top row** of panels shows hematoxylin and eosin staining (H&E) of the hippocampus region, **middle row** of panels shows immunohistochemical (IHC) staining of the VSV antigen in the hippocampus region, and **bottom row** of panels shows terminal transferase deoxyuridine triphosphate nick-end labeling (TUNEL) assay of the hippocampus. Adjacent brain sections were used. **Arrows** indicate the tumor.

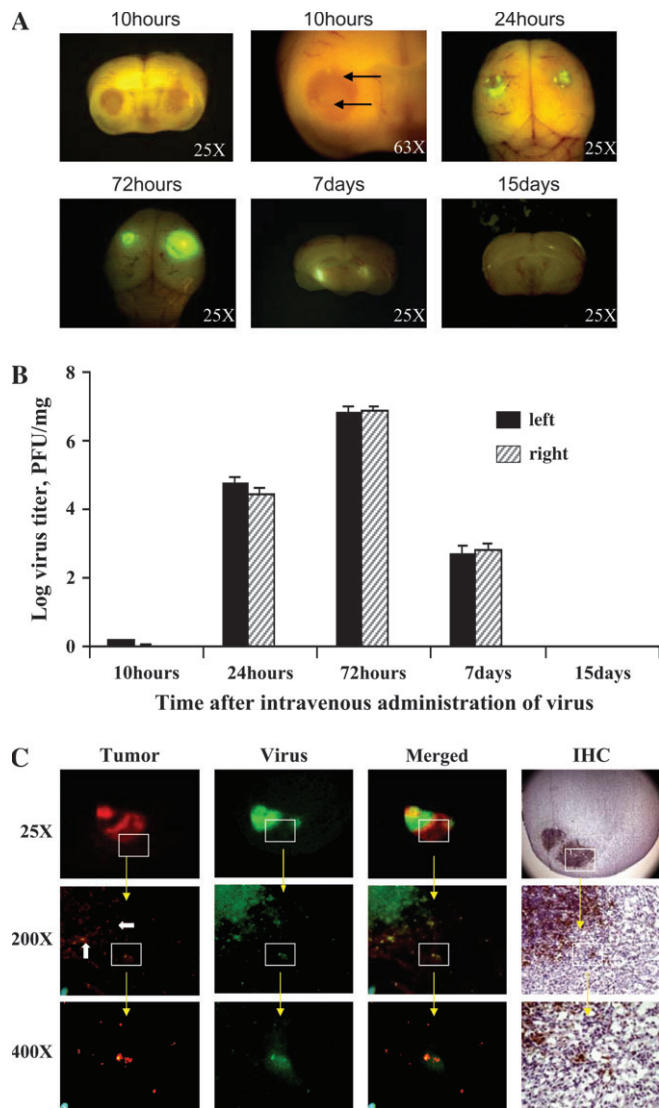


Fig. 6. Distribution of intravenously administered vesicular stomatitis virus strain $\Delta M51$ ($VSV^{\Delta M51}$) expressing green fluorescent protein (GFP) in multifocal gliomas and invasive tumor cells. Mice bearing intracerebral bilateral U87 tumors were treated intravenously with live or dead $VSV^{\Delta M51}$ virus. Mice were killed at several timepoints, and localization of tumor and virus was assessed. **A)** Photomicrograph of GFP-expressing virus in bilateral tumors. **Arrows** indicate GFP-virus expression. **B)** Titer of virus present in the bilateral tumors ($n = 3$ mice per time point). Tumors on each side of the brain were harvested for virus extraction, and the samples were analyzed by virus recovery assay. The **error bars** indicate upper 95% confidence intervals. **C)** Localization of $VSV^{\Delta M51}$ expression in experimental invasive gliomas using fluorescence microscopy and immunohistochemistry (IHC) VSV antigen staining. Mice bearing U87-RFP-labeled tumors were injected intravenously, via the tail vein, with a single dose of $VSV^{\Delta M51}$ and were killed 72 hours later. **Left three panels of the top row** show fluorescent images of a representative RFP-labeled tumor and GFP virus expression in frozen sections (magnification: $\times 25$); **left three panels of the center and bottom rows** show representative GFP virus targeting the invasive RFP-glioma cells (rows show increasing magnification of the same section: **top row**, $\times 25$; **center row**, $\times 200$; **bottom row**, $\times 400$). **White arrows** indicate the edge of the tumor. Merged refers to a superimposed image of tumor and virus (**third column**). IHC of $VSV^{\Delta M51}$ protein on consecutive sections (**right column**) confirms the presence of viral proteins in the invasive glioma cells (brown staining; magnification, top to bottom: $\times 25$, $\times 200$, $\times 400$).

Infection and Killing by $VSV^{\Delta M51}$ of Primary Human Malignant Gliomas Cultured From Surgical Specimens

We next determined whether the *in vitro* cell line results would also apply to glioma samples from patients. Accordingly, we

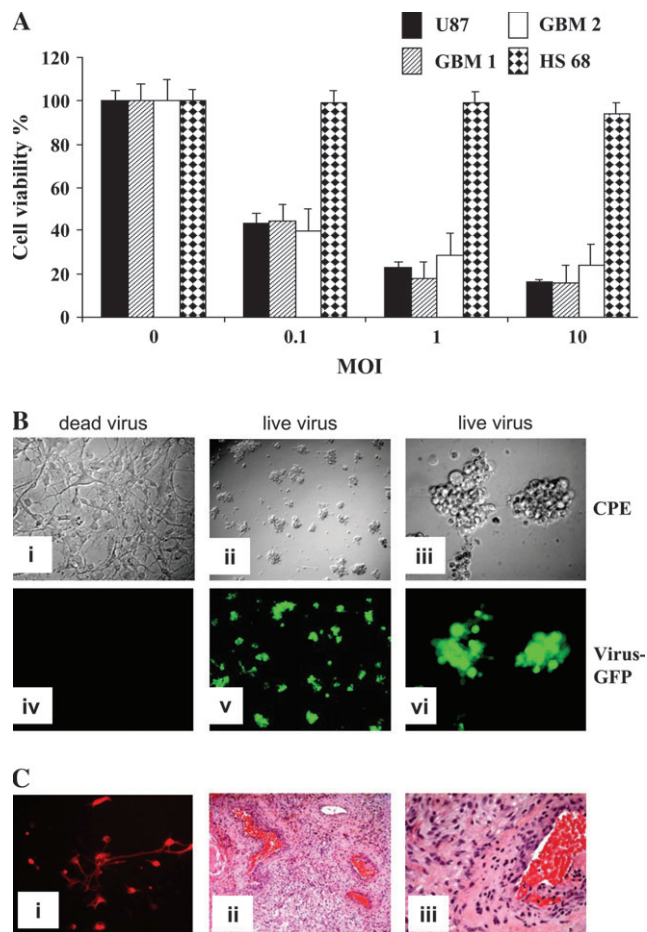


Fig. 7. Effect of vesicular stomatitis virus strain $\Delta M51$ ($VSV^{\Delta M51}$) on human primary tumor samples. **A)** The viability of the glioma samples was measured by the 3-(4,5-dimethylthiazol-2-yl)-2,5-diphenyl-2H-tetrazolium bromide assay, 72 hours after infection with $VSV^{\Delta M51}$ (0.1–10 multiplicity of infection). **Error bars** indicate 95% confidence intervals of three independent experiments performed in triplicate. Samples of dissociated tumor cells from a surgical sample of glioma were plated and 24 hours later infected with either live or dead virus. U87 malignant glioma and HS68 (nontransformed human fibroblasts) were used as positive and negative controls for $VSV^{\Delta M51}$ susceptibility. **B)** Virus infectivity and cell killing were confirmed by assessing the cytopathic effect (CPE) and virus green fluorescent protein (GFP) expression; shown are phase contrast (**upper panel**) and fluorescent GFP (**lower panel**) images from a representative human glioblastoma taken 24 hours after infection (magnification: **ii** and **v**, $\times 100$; **iii** and **vi**, $\times 400$). Dead virus was used as a negative control (**i** and **iv**, $\times 100$). **C)** Glial fibrillary acidic protein (**i**) and hematoxylin and eosin staining (**ii** and **iii**) of the same sample as above (magnification: **i**, $\times 400$; **ii**, $\times 100$; **iii**, $\times 400$).

tested whether $VSV^{\Delta M51}$ could infect and kill short-term glioma cultures derived from glioma surgical specimens. We examined the susceptibility to $VSV^{\Delta M51}$ of 15 *ex vivo* brain tumor surgical specimens derived from four glioblastomas, five oligodendrogliomas, five astrocytomas, and one gliosarcoma. All specimens tested (15/15) were killed by $VSV^{\Delta M51}$ infection (Fig. 7, A) and to a degree that was similar to infection and killing of U87. A widespread cytopathic effect and viral GFP expression was seen in live virus-treated glioma cells (Fig. 7, B-ii, iii, v, vi). In contrast, short-term cultures treated with dead virus showed no cytopathic effect or viral GFP expression (Fig. 7, B-i, iv). GFAP staining confirmed the glial lineage of the astrocytic specimens (e.g., a glioblastoma) (Fig. 7, C-i), which was also apparent morphologically using hematoxylin and eosin staining (Fig. 7, C-ii, iii).

DISCUSSION

We found that an attenuated VSV mutant, designated VSV Δ M51, infected and killed all malignant glioma cell lines tested and did not infect normal cells in vitro. When administered intravenously to CD-1 nude mice bearing human gliomas, VSV Δ M51 dramatically prolonged their survival and infected both multifocal gliomas and invasive glioma cells. The invasive and multifocal natures of glioma are major clinical challenges in treating this disease.

An ideal oncolytic virus for cancer should have several characteristics (38,42,59). It should have effective delivery into multiple sites within the tumor, evade innate and acquired immune responses, produce rapid viral replication, spread within the tumor, and infect multifocal tumors. It should also be “engineerable” so that it can be modified to, for example, improve its efficacy or tumor targeting. This is precisely what we found using the attenuated live virus we constructed (VSV Δ M51). Its efficacy was maintained and the antiviral responses were enhanced in normal cells, thereby improving its therapeutic index (43). In addition, we found that VSV Δ M51 infects both multifocal gliomas and invasive glioma cells. Conventional therapies such as surgery and radiotherapy are ineffective in treating invasive glioma cells because these cells may have become more resistant to these therapies than the tumor cells in the main tumor mass by adopting a number of cellular characteristics (e.g., increasing expression of survival pathways, decreasing expression of apoptotic programs, reduced proliferation, etc.) (60). Hence, VSV Δ M51 may represent an effective treatment for these chemotherapy-resistant tumor cells.

We compared the effectiveness and toxicities of VSV Δ M51 to reovirus in this study on the basis of our previous work (8,9,55). We found that VSV Δ M51 was superior in several ways to reovirus for treating gliomas. VSV Δ M51 killed all glioma lines we tested (including two that were resistant to reovirus), was effective in vivo when administered systemically, infected invasive glioma cells, and killed multifocal gliomas. By contrast, reovirus did not cause regression of bilateral gliomas in an immunocompetent rat glioma model (55). However, reovirus is superior to VSV Δ M51 in many other ways. When administered intratumorally, reovirus “cures” experimental gliomas in the majority of glioma-bearing mice (i.e., mice survived until the experiment was arbitrarily terminated 90 days after tumor implantation, often without histologic evidence of residual tumor) (8), whereas we found that intravenous VSV Δ M51 did not cure any mice. Finally, unlike VSV Δ M51, reovirus is benign when administered intracerebrally in adult nude mice (8) or immunocompetent rats (55). Comparisons between oncolytic viruses of putative efficacy or toxicities in animal models at present are very limited (61). Definitive conclusions regarding efficacy or toxicity await the testing of these oncolytic viruses in clinical trials in malignant glioma patients.

Our study has several limitations. First, we have not yet evaluated VSV Δ M51 in immunocompetent models of gliomas. Such evaluation is important because immune responses (partially ablated in the immunocompromised mice we used here) may limit delivery of the virus to the tumor when administered intravenously. Immune responses may also limit the distribution of the virus within the tumor. Second, the precise mechanism by which intravenous VSV Δ M51 accesses the invasive glioma cells, which in many cases appear to be single cells, is unknown. The

main tumor mass of U87 is highly vascularized and has a “leaky” blood–brain barrier, which would allow intravenously delivered virus access to the main tumor mass (62,63). In contrast, invasive glioma cells are not believed to be extensively vascularized (64) and would therefore have limited contact with systemically delivered virus. We assume that higher pressure within the tumor mass (65) and high concentrations of virus within the tumor, under pressure, may move the virus out along tracts of white matter. Because these invasive cells may be in a hypoxic environment, it should be noted that VSV is able to infect and kill hypoxic glioma cells both in vitro and in vivo (24). Alternatively, peritumoral increases in neovascularity and tissue edema can increase the permeability of the blood–brain barrier (66,67), allowing the virus to leak out into the perivascular interstitium around the vessels. Third, all the glioma-bearing mice ultimately died from recurrent tumor. We are now exploring strategies to understand the causes of treatment failure with the goal of improving its efficacy (e.g., using live imaging of viral delivery, improving blood–brain barrier breakdown and intra-arterial delivery, etc.).

REFERENCES

- (1) Scott JN, Rewcastle NB, Brasher PM, Fulton D, Mackinnon JA, Hamilton M, et al. Which glioblastoma multiforme patient will become a long-term survivor? A population-based study. *Ann Neurol* 1999;46:183–8.
- (2) Stupp R, Mason WP, van den Bent MJ, Weller M, Fisher B, Taphoorn MJ, et al. Radiotherapy plus concomitant and adjuvant temozolomide for glioblastoma. *N Engl J Med* 2005;352:987–96.
- (3) Fisher PG, Buffler PA. Malignant gliomas in 2005: where to GO from here? *JAMA* 2005;293:615–7.
- (4) Ohgaki H, Kleihues P. Epidemiology and etiology of gliomas. *Acta Neuropathol (Berl)* 2005;109:93–108.
- (5) Castro MG, Cowen R, Williamson IK, David A, Jimenez-Dalmaroni MJ, Yuan X, et al. Current and future strategies for the treatment of malignant brain tumors. *Pharmacol Ther* 2003;98:71–108.
- (6) Giese A, Bjerkvig R, Berens ME, Westphal M. Cost of migration: invasion of malignant gliomas and implications for treatment. *J Clin Oncol* 2003;21:1624–36.
- (7) Yang WQ, Senger D, Muzik H, Shi ZQ, Johnson D, Brasher PM, et al. Reovirus prolongs survival and reduces the frequency of spinal and leptomeningeal metastases from medulloblastoma. *Cancer Res* 2003;63:3162–72.
- (8) Wilcox ME, Yang WQ, Senger D, Rewcastle NB, Morris DG, Brasher PM, et al. Reovirus as an oncolytic agent against experimental human malignant gliomas. *J Natl Cancer Inst* 2001;93:903–12.
- (9) Coffey MC, Strong JE, Forsyth PA, Lee PW. Reovirus therapy of tumors with activated Ras pathway. *Science* 1998;282:1332–4.
- (10) Todo T, Rabkin SD, Sundaresan P, Wu A, Meehan KR, Herscovitz HB, et al. Systemic antitumor immunity in experimental brain tumor therapy using a multimitated, replication-competent herpes simplex virus. *Hum Gene Ther* 1999;10:2741–55.
- (11) Mineta T, Rabkin D, Yazaki T, Hunter WD, Martuza RL. Attenuated multimitated herpes simplex virus-1 for the treatment of malignant gliomas. *Nat Med* 1995;1:938–43.
- (12) Yazaki T, Manz HJ, Rabkin SD, Martuza RL. Treatment of human malignant meningiomas by G207, a replication-competent multimitated herpes simplex virus 1. *Cancer Res* 1995;55:4752–6.
- (13) Mineta T, Rabkin SD, Martuza RL. Treatment of malignant gliomas using ganciclovir-hypersensitive, ribonucleotide reductase-deficient herpes simplex viral mutant. *Cancer Res* 1994;54:3963–6.
- (14) Martuza RL, Malick A, Markert JM, Ruffner KL, Coen DM. Experimental therapy of human glioma by means of a genetically engineered virus mutant. *Science* 1994;252:854–6.
- (15) Csatory LK, Gosztonyi G, Szeberenyi J, Fabian Z, Liszha V, Bodey B, et al. MTH-68/H oncolytic viral treatment in human high-grade gliomas. *J Neurooncol* 2004;67:83–93.

- (16) Csatory LK, Bakacs T. Use of Newcastle disease virus vaccine (MTH-68/H) in a patient with high-grade glioblastoma. *JAMA* 2000;283:2107.
- (17) Freeman AI, Zakay-Rones Z, Gomori JM, Linetsky E, Rasooly L, Greenbaum E, et al. Phase I/II trial of intravenous NDV-HUJ oncolytic virus in recurrent glioblastoma multiforme. *Mol Ther* 2005;13:221–8.
- (18) Gromeier M, Lachmann S, Rosenfeld MR, Gutin PH, Wimmer E. Intergenic poliovirus recombinants for the treatment of malignant glioma. *Proc Natl Acad Sci U S A* 2000;97:6803–8.
- (19) Ochiai H, Moore SA, Archer GE, Okamura T, Chewing TA, Marks JR, et al. Treatment of intracerebral neoplasia and neoplastic meningitis with regional delivery of oncolytic recombinant poliovirus. *Clin Cancer Res* 2004;10:4831–8.
- (20) Lun XQ, Yang WQ, Alain T, Shi ZQ, Muzik H, Barrett JW, et al. Myxoma virus is a novel oncolytic virus with significant antitumor activity against experimental human gliomas. *Cancer Res* 2005;65:9982–90.
- (21) Chiocca EA, Abbed KM, Tatter S, Louis DN, Hochberg F, Kracher J, et al. A phase I open-label, dose-escalation, multi-institutional trial of injection with an E1B-attenuated adenovirus, ONYX-015, into the peritumoral region of recurrent malignant gliomas, in the adjuvant setting. *Mol Ther* 2004;10:958–66.
- (22) Jiang H, Conrad C, Fueyo J, Gomez-Manzano C, Liu TJ. Oncolytic adenoviruses for malignant glioma therapy. *Front Biosci* 2003;8:d577–88.
- (23) Georger B, Grill J, Opolon P, Morizet J, Aubert G, Terrier-Lacombe MJ, et al. Oncolytic activity of the E1B-55 kDa-deleted adenovirus ONYX-015 is independent of cellular p53 status in human malignant glioma xenografts. *Cancer Res* 2002;62:764–72.
- (24) Connor JH, Naczki C, Koumenis C, Lyles DS. Replication and cytopathic effect of oncolytic vesicular stomatitis virus in hypoxic tumor cells in vitro and in vivo. *J Virol* 2004;78:8960–70.
- (25) Porosnicu M, Mian A, Barber GN. The oncolytic effect of recombinant vesicular stomatitis virus is enhanced by expression of the fusion cytosine deaminase/uracil phosphoribosyltransferase suicide gene. *Cancer Res* 2003;63:8366–76.
- (26) Balachandran S, Porosnicu M, Barber GN. Oncolytic activity of vesicular stomatitis virus is effective against tumors exhibiting aberrant p53, Ras, or Myc function and involves the induction of apoptosis. *J Virol*. 2001;75:3474–9.
- (27) Lee H, Song JJ, Kim E, Yun CO, Choi J, Lee B, et al. Efficient gene transfer of VSV-G pseudotyped retroviral vector to human brain tumor. *Gene Ther* 2001;8:268–73.
- (28) Balachandran S, Barber GN. Vesicular stomatitis virus (VSV) therapy of tumors. *IUBMB Life* 2000;50:135–8.
- (29) Lang FF, Bruner JM, Fuller GN, Aldape K, Prados MD, Chang S, et al. Phase I trial of adenovirus-mediated p53 gene therapy for recurrent glioma: biological and clinical results. *J Clin Oncol* 2003;21:2508–18.
- (30) Hermiston TW, Kuhn I. Armed therapeutic viruses: strategies and challenges to arming oncolytic viruses with therapeutic genes. *Cancer Gene Ther* 2002;9:1022–35.
- (31) Green NK, Seymour LW. Adenoviral vectors: systemic delivery and tumor targeting. *Cancer Gene Ther* 2002;9:1036–42.
- (32) Yamamoto S, Yoshida Y, Aoyagi M, Ohno K, Hirakawa K, Hamada H. Reduced transduction efficiency of adenoviral vectors expressing human p53 gene by repeated transduction into glioma cells in vitro. *Clin Cancer Res* 2002;8:913–21.
- (33) Harrow S, Papanastassiou V, Harland J, Mabbs R, Petty R, Fraser M, et al. HSV1716 injection into the brain adjacent to tumor following surgical resection of high-grade glioma: safety data and long-term survival. *Gene Ther* 2004;11:1648–58.
- (34) Papanastassiou V, Rampling R, Fraser M, Petty R, Hadley D, Nicoll J, et al. The potential for efficacy of the modified (ICP 34.5(-)) herpes simplex virus HSV1716 following intratumoral injection into human malignant glioma: a proof of principle study. *Gene Ther* 2002;9:398–406.
- (35) Markert JM, Medlock MD, Rabkin SD, Gillespie GY, Todo T, Hunter WD, et al. Conditionally replicating herpes simplex virus mutant, G207 for the treatment of malignant glioma: results of a phase I trial. *Gene Ther* 2000;7:867–74.
- (36) Rampling R, Cruickshank G, Papanastassiou V, Nicoll J, Hadley D, Brennan D, et al. Toxicity evaluation of replication-competent herpes simplex virus (ICP 34.5 null mutant 1716) in patients with recurrent malignant glioma. *Gene Ther* 2000;7:859–66.
- (37) Forsyth PA, Roldan G, George D, Wallace C, Morris DG, Cairncross J, et al. A phase I trial of intratumoral (i.t.) administration of reovirus in patients with histologically confirmed recurrent malignant gliomas (MGs). *J Clin Oncol ASCO Proc* 2006;24:18S (June 20 Supplement), Abstract 1563.
- (38) Parato K, Senger D, Forsyth PA, Bell JC. Recent progress in the battle between oncolytic viruses and tumors. *Nat Rev Cancer* 2005;5:965–76.
- (39) Barber GN. Vesicular stomatitis virus as an oncolytic vector. *Viral Immunol* 2004;17:516–27.
- (40) Bell JC, Lichty B, Stojdl D. Getting oncolytic virus therapies off the ground. *Cancer Cell* 2003;4:7–11.
- (41) Gromeier M, Wimmer E. Viruses for the treatment of malignant glioma. *Curr Opin Mol Ther* 2001;3:503–8.
- (42) Kirn D, Martuza RL, Zwiebel J. Replication-selective virotherapy for cancer: biological principles, risk management and future directions. *Nat Med* 2001;7:781–7.
- (43) Stojdl DF, Lichty BD, TenOever BR, Paterson JM, Power AT, Knowles S, et al. VSV strains with defects in their ability to shutdown innate immunity is potent systemic anti-cancer agents. *Cancer Cell* 2003;4:263–75.
- (44) Stojdl DF, Lichty B, Knowles S, Marius R, Atkins H, Sonenberg N, et al. Exploiting tumor-specific defects in the interferon pathway with a previously unknown oncolytic virus. *Nat Med* 2000;6:821–5.
- (45) Balachandran S, Barber N. Defective translational control facilitates vesicular stomatitis virus oncolysis. *Cancer Cell* 2004;5:51–65.
- (46) Liu R, Varghese S, Rabkin SD. Oncolytic herpes simplex virus vector therapy of breast cancer in C3(1)/SV40 T-antigen transgenic mice. *Cancer Res* 2005;65:1532–40.
- (47) Abe T, Wakimoto H, Bookstein R, Maneval DC, Chiocca EA, Basilion JP. Intra-arterial delivery of p53-containing adenoviral vector into experimental brain tumors. *Cancer Gene Ther* 2002;9:228–35.
- (48) Ikeda K, Wakimoto H, Ichikawa T, Jung S, Hochberg FH, Louis DN, et al. Complement depletion facilitates the infection of multiple brain tumors by an intravascular, replication-conditional herpes simplex virus mutant. *J Virol* 2000;74:4765–75.
- (49) Schellingerhout D, Rainov NG, Breakefield XO, Weissleder R. Quantitation of HSV mass distribution in a rodent brain tumor model. *Gene Ther* 2000;7:1648–55.
- (50) Ikeda K, Ichikawa T, Wakimoto H, Silver JS, Deisboeck TS, Finkelstein D, et al. Oncolytic virus therapy of multiple tumors in the brain requires suppression of innate and elicited antiviral responses. *Nat Med* 1999;5:881–7.
- (51) Zhan JH, Gao Y, Wang W, Shen A, Aspelund A, Young M, et al. Tumor-specific intravenous gene delivery using oncolytic adenoviruses. *Cancer Gene Ther* 2005;12:19–25.
- (52) LeMay DR, Kittaka M, Gordon EM, Gray B, Stins MF, McComb JG, et al. Intravenous RMP-7 increases delivery of ganciclovir into rat brain tumors and enhances the effects of herpes simplex virus thymidine kinase gene therapy. *Hum Gene Ther* 1998;9:989–95.
- (53) Ebert O, Harbaran S, Shinozaki K, Woo SL. Systemic therapy of experimental breast cancer metastases by mutant vesicular stomatitis virus in immune-competent mice. *Cancer Gene Ther* 2005;12:350–8.
- (54) Shinozaki K, Ebert O, Woo SL. Treatment of multi-focal colorectal carcinoma metastatic to the liver of immune-competent and syngeneic rats by hepatic artery infusion of oncolytic vesicular stomatitis virus. *Int J Cancer* 2005;114:659–64.
- (55) Yang WQ, Lun XQ, Palmer CA, Wilcox ME, Muzik H, Shi ZQ, et al. Efficacy and safety evaluation of human reovirus type 3 in immunocompetent animals: racine and nonhuman primates. *Clin Cancer Res* 2004;10:8561–76.
- (56) Yang WQ, Senger DL, Lun XQ, Muzik H, Shi ZQ, Dyck RH, et al. Reovirus as an experimental therapeutic for brain and leptomeningeal metastases from breast cancer. *Gene Ther* 2004;11:1579–89.
- (57) Chomczynski P, Sacchi N. Single-step method of RNA isolation by acid guanidinium thiocyanate-phenol-chloroform extraction. *Anal Biochem* 1987;162:156–9.
- (58) Cave DR, Hendrickson FM, Huang AS. Defective interfering virus particles modulate virulence. *J Virol* 1985;55:366–73.
- (59) Wein LM, Wu JT, Kirn DH. Validation and analysis of a mathematical model of a replication-competent oncolytic virus for cancer treatment: implications for virus design and delivery. *Cancer Res* 2003;63:1317–24.
- (60) Joy AM, Beaudry CE, Tran NL, Ponce FA, Holz DR, Demuth T, et al. Migrating glioma cells activate the PI3-K pathway and display decreased susceptibility to apoptosis. *J Cell Sci* 2003;116:4409–17.

- (61) Wollmann G, Tattersall P, van den Pol AN. Targeting human glioblastoma cells: comparison of nine viruses with oncolytic potential. *J Virol* 2005;79:6005–22.
- (62) Yuan F, Salehi HA, Boucher Y, Vasthare US, Tuma RF, Jain RK. Vascular permeability and microcirculation of gliomas and mammary carcinomas transplanted in rat and mouse cranial windows. *Cancer Res* 1994;54:4564–8.
- (63) Kragh M, Quistorff B, Lund EL, Kristjansen PE. Quantitative estimates of vascularity in solid tumors by non-invasive near-infrared spectroscopy. *Neoplasia* 2001;3:324–30.
- (64) Stewart PA, Hayakawa K, Farrell CL, Del Maestro RF. Quantitative study of microvessel ultrastructure in human peritumoral brain tissue. Evidence for a blood-brain barrier defect. *J Neurosurg* 1987;67:697–705.
- (65) Helmlinger G, Yuan F, Dellian M, Jain RK. Interstitial pH and pO₂ gradients in solid tumors in vivo: high-resolution measurements reveal a lack of correlation. *Nat Med* 1997;3:177–82.
- (66) Jain RK. 1995 Whitaker lecture: delivery of molecules, particles, and cells to solid tumors. *Ann Biomed Eng* 1996;24:457–73.
- (67) Yuan F, Chen Y, Dellian M, Safabakhsh N, Ferrara N, Jain RK. Time-dependent vascular regression and permeability changes in established

human tumor xenografts induced by an anti-vascular endothelial growth factor/vascular permeability factor antibody. *Proc Natl Acad Sci U S A* 1996; 93:14765–70.

NOTES

This work was funded by the National Cancer Institute of Canada with funds raised by the Canadian Cancer Society (D. Stojdl and P. A. Forsyth), a Program Project Grant from the Terry Fox Foundation (J. C. Bell and P. A. Forsyth), and the Clark Smith Integrative Brain Tumor Research Center (P. A. Forsyth and D. L. Senger). T. Alain is funded by the Alberta Heritage Foundation for Medical Research and a fellowship by the Canadian Institutes of Health Research. The sponsors had no role in the design, analysis, writing, or decision to submit the study for publication.

Funding to pay the Open Access publication charges for this article was provided by the Clark Smith Integrative Brain Tumor Center.

Manuscript received December 16, 2005; revised August 18, 2006; accepted September 8, 2006.